ROYAL SOCIETY OF CHEMISTRY

PAPER

Check for updates

Poly(trimethylene carbonate-*co*-valerolactone) copolymers are materials with tailorable properties: from soft to thermoplastic elastomers†

Lucie Reinišová [ID] and Soňa Hermanová [ID] *

Aliphatic poly(ester-carbonates) are receiving extensive research attention as tailorable materials suitable for multiple applications from tissue engineering and 3D scaffold printing to drug delivery. Thus, simple reliable procedures for producing easily tailorable poly(ester-carbonates) without metal residues are continuously sought after. In this work, we report on one-pot synthesis of random copolymers of TMC and δ-VL using metal-free biocompatible 1,5,7-triazabicyclo[4.4.0]dec-5-ene as a catalyst and benzyl alcohol and poly(ethylene oxide) as initiators. Random poly(ester-carbonates) with TMC : VL unit ratios ranging from 80 : 20 to 20 : 80 were synthesized *via* ring-opening polymerization while displaying excellent agreement of comonomers' ratios in the feed and copolymer chains. The copolymers' supramolecular structure, thermal and mechanical properties were thoroughly analyzed by various methods. The obtained results clearly indicated that the physicochemical properties can be controlled simply by varying the ratio of comonomers and the length of segments in the copolymer chain. Several copolymers exhibited behavior of thermoplastic elastomers with the most promising one exhibiting a 2200% increase in elongation at break compared to the poly(valerolactone) homopolymer while retaining tensile strength and Young's modulus suitable for biomedical applications. Overall, our work contributed to widening the portfolio of tailorable copolymers for specialized bioapplications and possibly paving a way for the use of more sustainable polymers in the biomedical field.

Introduction

Over the years, aliphatic polyesters, polycarbonates, and their copolymers have become some of the most intensively used biodegradable polymers in the medical field.[1,2] This trend isn't surprising, as it mirrors their high application potential, since these polymers offer a wide variety of properties achievable simply by changing their molar mass, comonomer ratio and/or microstructure.[3–5] Among them, biodegradable and biocompatible copolymers of trimethylene carbonate (TMC) and ε-caprolactone (ε-CL) have been steadily gaining interest due to their capability to be easily processed into 3D porous structures like scaffolds, films and fibers[6–10] and for their possible application in nerve tissue regeneration.[11]

These copolymers are predominantly obtained by ring-opening copolymerization (ROCOP) of their cyclic monomers using tin(II) 2-ethylhexanoate (Sn(Oct)$_2$) as a catalyst both in laboratory and commercial scale. However, the presence of tin residues in the final material presents a health risk and its

amount in the polymer cannot exceed 50 ppm for certain applications.[12,13] Also, Sn(Oct)$_2$ was reported as cytotoxic and could potentially decrease cell viability in tissue engineered products.[12] Therefore, metal-free catalytic systems with higher biocompatibility and control over obtained copolymer microstructure are continuously sought after.[14–17]

Multiple organocatalysts have shown high promise in obtaining tailored biocompatible polymer materials, with the most perspective being proton-donating compounds (Brönsted acids), strong bases (amidine, guanidine), nucleophiles and hydrogen-bond forming systems.[18,19] These systems are also suitable for synthesis of tailored copolymers, since by selecting a specific catalyst/comonomer combination, it is possible to obtain various desired architectures, such as random, gradient and block copolymers.[14,20] This possibility has been also utilized for ROCOP of TMC or its derivates with cyclic lactones producing poly(ester-carbonates).[21–23]

Several organocatalysts gained interest as prospective systems for obtaining poly(ester-carbonate) copolymers with diverse microstructures, such as diphenyl phosphate (DPP)[10,24] or methanesulfonic acid (MSA).[25] Besides these compounds, triazabicyclo[4.4.0]dec-5-ene (TBD), a Brönsted base, has received considerable interest in the recent years. This versatile catalyst is highly active in ring-opening (co)polymerizations of

Department of Polymers, Faculty of Chemical Technology, University of Chemistry and Technology Prague, Technická 5, 16628 Prague, Czech Republic. E-mail: sona. hermanova@vscht.cz

various cyclic compounds, such as carbonates, lactones, lactides, carbosiloxanes over a wide temperature range.[26,27]

Besides its versatility and high activity towards various cycles, another advantage over other organocatalysts lies in its capability to produce copolymers with various microstructures. It has been reported as a suitable organocatalyst for obtaining multiblock[22] and random[23,28] poly(ester-carbonate) copolymers. TBD is also selective towards six-membered rings and exhibits higher activity towards cyclic carbonates than lactones.[29] This attribute was exploited for ROCOP of six membered cyclic carbonate (2-allyloxymethyl-2-ethyl-trimethylene carbonate) (AOMEC) and ε-CL. The multiblock PCL-*b*-P(AOMEC) copolymers were synthesized by temperature-dependent on/off switch. The polymerization of ε-CL was periodically stopped by decreasing the temperature from 30 °C to −40 °C, while the propagation of added AOMEC proceeded.[22] TBD was also reported to be a highly active catalyst in ROCOP of dimethylacetal dihydroxyacetone carbonate (MeO$_2$DHAC) and ε-CL producing random copolymers with good agreement of the chain unit ratio with the feed ratio.[23] Random copolymers of TMC and six-membered δ-VL (TMC : VL = 50 : 50) were synthesized by Nederberg *et al.* with quantitative conversion of both comonomers.[28]

Sadly, even though δ-VL exhibits higher reactivity and better reaction control than ε-CL in TBD-catalyzed polymerizations,[6–9] its copolymers with TMC have received less attention as potential advanced biomaterials than P(TMC-CL) copolymers. When utilizing TBD as catalyst it should be possible to obtain higher molar mass P(TMC-VL) copolymers with tailored microstructure for various bioapplications. Furthermore, δ-VL and its derivates are easily accessible from renewable sources, making the copolymers sustainable.[30,31]

In this work we synthesized P(TMC-*co*-VL) and PEO-*b*-P(TMC-*co*-VL) copolymers with various TMC : VL unit ratios using TBD as a catalyst. We further analyzed the influence of comonomer ratio on copolymer microstructure, thermal and mechanical properties and discussed their suitability for biomedical applications.

Experimental

Materials

Trimethylene carbonate (TMC, Labso Chimie, France) was twice recrystallized from diethyl ether, δ-valerolactone (δ-VL, TCI Europe) was dried over CaH$_2$ and freshly distilled prior to polymerization. Methoxy poly(ethylene oxide) (mPEO-OH, M_w = 5 kg mol^{-1}, Đ = 1.12), benzyl alcohol (BnOH), and 1,5,7-triazabicyclo [4.4.0]dec-5-ene (TBD) were purchased from Sigma Aldrich. TBD was used as received. BnOH was dried with calcium oxide followed by vacuum distillation and stored over molecular sieves. mPEO-OH was dissolved in dichloromethane, precipitated in diethyl ether and dried under vacuum until constant weight. Dichloromethane (DCM, Penta, CZ) was dried over CaH$_2$ and distilled prior to use. Sodium chloride (Lachema, CZ), sodium hydrogen carbonate (Lachema, CZ), potassium chloride (Lachema, CZ), di-potassium hydrogen phosphate trihydrate (Lachema, CZ), magnesium chloride (Lachema, CZ), calcium chloride (Lachema, CZ), sodium sulfate (Penta, CZ), tris-

hydroxymethyl aminomethane (Sigma-Aldrich, Germany) and hydrochloric acid (Penta, CZ) were all used as received.

Synthesis of copolymers and their characterization

All procedures were carried out under argon atmosphere using standard Schlenk techniques.

Polymerization reactions were performed in DCM solution according to a modified procedure based on works of Pratt and Nederberg *et al.*[28,32] All the runs were carried out for 1 h at room temperature, after which benzoic acid was added as a termination agent.

^{1}H and ^{13}C-NMR spectroscopy analyses of prepared copolymers were performed on Bruker Avance III™ at 500 MHz and Bruker 600 Avance III at 126 MHz, respectively. The analyses were conducted at 25 °C in CDCl$_3$. The data were interpreted according to Nederberg and Liu *et al.*[28] using MestReNova software. Representative poly(ester-carbonate) sample data are as follows: ^{1}H NMR of P(TMC-*co*-VL), CDCl$_3$: δ = 1.66–1.75 ppm (m, 4H, –CH$_2$CH$_2$–), δ = 1.95–2.10 ppm (m, 2H, –CH$_2$–), δ = 2.34 ppm (m, 2H, –OCOCH$_2$–), δ = 3.68 ppm (t, 2H, –CH$_2$OH VL α-end), δ = 3.72 ppm (t, 2H, –CH$_2$OH TMC α-end), δ = 4.05–4.16 ppm (m, 2H, –H$_2$COCO–), δ = 4.16–4.27 ppm (m, 4H, –H$_2$COCOOH$_2$–), δ = 5.12 ppm (s, 2H, ArCH$_2$OCO– ω-end), δ = 5.16 ppm (s, 2H, ArCH$_2$-OCOO– ω-end), δ = 7.32–7.40 ppm (m, 5H, aromatic).

^{1}H NMR of PEO-*b*-P(TMC-*co*-VL), CDCl$_3$: δ = 1.64–1.75 ppm (m, 4H, –CH$_2$CH$_2$–), δ = 1.97–2.10 ppm (m, 2H, –CH$_2$–), δ = 2.34 ppm (m, 2H, –OCOCH$_2$–), δ = 3.65 ppm (s, 4H, –CH$_2$O–), δ = 3.68 ppm (t, 2H, –CH$_2$OH VL α-end), δ = 3.72 ppm (t, 2H, –CH$_2$OH TMC α-end), δ = 3.79 ppm (s, 3H, –CH$_2$O–), δ = 4.05–4.16 ppm (m, 2H, –H$_2$COCO–), δ = 4.16–4.27 ppm (m, 4H, –H$_2$COCOOH$_2$–).

^{13}C {^{1}H} NMR of P(TMC-*co*-VL), CDCl$_3$: δ = 20.89–21.89 ppm, δ = 27.61–28.44 ppm, δ = 32.78–34.14 ppm, δ = 61.66–65.42 ppm, δ = 154.81–155.31 ppm, δ = 172.93–173.45 ppm.

Homo- or heterodiad content in the copolymer chains was calculated according to formulas adapted from Ling *et al.*[33] (eqn (1)). Eqn (1) shows the calculation of homo/heterodiad content in the copolymer chain from ^{1}H NMR peak intensities: (a) TMC–TMC homodiad (%), (b) VL–VL homodiad (%), (c) TMC–VL, VL–TMC heterodiads (%).

$$X_{TMC-TMC} = \frac{\dfrac{I_{4.24} - I_{4.14}}{2}}{\dfrac{I_{4.24} - I_{4.14}}{2} + I_{4.08} + I_{4.14} + I_{4.17}} \times 100 \quad (a)$$

$$X_{VL-VL} = \frac{I_{4.08}}{\dfrac{I_{4.24} - I_{4.14}}{2} + I_{4.08} + I_{4.14} + I_{4.17}} \times 100 \quad (b)$$

$$X_{heterodiads} = \frac{I_{4.14} + I_{4.17}}{\dfrac{I_{4.24} - I_{4.14}}{2} + I_{4.08} + I_{4.14} + I_{4.17}} \times 100 \quad (c)$$

The average sequence length of TMC or VL sequences in the copolymer chain (L_A^{TMC}, L_A^{VL}) was determined by using the following formulas adapted from Ling and Pêgo *et al.*[33,34] (eqn (2)). Eqn (2) shows the calculation of average sequence length in

the copolymer chain: (a) TMC sequence length, (b) VL sequence length.

$$L_A^{TMC} = \frac{\frac{I_{4.24} - I_{4.14}}{2}}{I_{4.17}} + 1 \qquad (a)$$

$$L_A^{VL} = \frac{I_{4.08}}{I_{4.14}} + 1 \qquad (b)$$

For the PEO-b-P(TMC-co-VL) copolymers, the number was determined for the P(TMC-co-VL) block.

Number average molar mass was calculated from ^1H NMR spectroscopy (CDCl$_3$) according to integral ratio of peaks by eqn (3a–d). Eqn (3) shows the molar mass determination from ^1H NMR spectroscopy: (a) M_n^{PVL}, (b) $M_n^{(PEO-b-PVL)}$, (c) $M_n^{(PEO-b-PTMC)}$, (d) $M_n^{(PEO-b-P(TMC-co-VL))}$.

$$M_n^{PVL} = \left(\frac{I_{4.08}}{\frac{I_{5.12} + I_{3.65}}{2}} + 1 \right) \times 100.117 + 108.14 \qquad (a)$$

$$M_n^{PEO-b-PVL} = \frac{I_{2.27}}{I_{3.57}} \times 2 \times DP_{PEO} \times 100.12 + M_n^{PEO} \qquad (b)$$

$$M_n^{PEO-b-PTMC} = \frac{I_{1.98}}{I_{3.57}} \times 2 \times DP_{PEO} \times 102.09 + M_n^{PEO} \qquad (c)$$

$$M_n^{PEO-b-P(TMC-co-VL)} = \left(\frac{I_{2.27}}{I_{3.57}} \times 2 \times DP_{PEO} \times 100.12 \right) + M_n^{PEO} + \left(\frac{I_{1.98}}{I_{3.57}} \times 2 \times DP_{PEO} \times 102.09 \right) \qquad (d)$$

Attenuated Total Reflectance-Fourier Transform Infrared (ATR-FTIR) spectra of copolymers were obtained on Nicolet iS50R FT-IR spectrometer (Thermo-Nicolet, USA). Spectra were recorded at 4 cm^{-1} resolution with 128 scans and scan range 4000 to 400 cm^{-1}.

SEC analysis was utilized to determine apparent number-average molar mass (M_n), apparent weight-average molar mass (M_w), and dispersity Đ (M_w/M_n). Measurements were carried out on SEC Waters Breeze chromatograph equipped with two PSS Lux LIN M 5 μm (7.8 mm × 300 mm) columns and a refractive index detector (RI 880 nm) using polystyrene calibration. Mobile phase (THF) flow was 1 mL min^{-1} and analysis temperature was 35 °C.

Wide-angle X-ray diffraction (WAXD) was used to determine phase composition. The analyses were performed on XRD PANanalytical X'Pert PRO diffractometer at 25 °C using CuKα radiation (40 kV, 30 mA) with step size 0.0390° 2θ and 5.0187–59.9307° 2θ angle range. Thermal properties were measured by differential scanning calorimetry (DSC) on Q200 Differential Scanning Calorimeter (TA Instruments) under nitrogen flow (50 mL min^{-1}) at scanning rate of 5 min^{-1}.

Copolymer mechanical properties

To evaluate mechanical properties, copolymer films (thickness ~0.1 mm) were prepared via solution casting. The copolymers were dissolved in DCM (10% w/v) and casted on a glass or PTFE dish. The films were dried at 25 °C for 48 h. Stress strain measurements were performed on Instron 3365 uniaxial testing machine (Instron, USA) according to EN ISO 527-1/2. The testing specimens were die-cut by a 5B type dog-bone cut head. The specimens were either tested directly or after 48 h-incubation at 37 °C in simulated body fluid (SBF, pH = 7.4), prepared according to Kokubo et al.[35] The measurement was performed at room temperature with crosshead speed set at 50 mm min^{-1}, fivefold for each sample. The incubated specimens were tested directly after removing from SBF.

The temperature influence on dynamic mechanical properties was analyzed by dynamic mechanical analysis (DMA) on DMA DX04T (RMI, CZ) dynamic mechanical analyzer. The specimens were prepared by cutting copolymer films into 10 × 5 × 0.1 mm strips. The measurements were performed in sinusoidal mode at temperature range −80 to 80 °C, at 3 °C min^{-1} heating rate. The applied frequency was set at 10 Hz and force amplitude at 200 mN.

The morphology of representative films was observed by Leica DM 6000B polarization optical microscope (Leica Microsystems GmbH, Germany) at 20× magnification.

Results and discussion

In green polymerization chemistry, TBD is recognized as a unique versatile organocatalyst for efficient ring-opening (co) polymerizations (ROCOP, ROP) of cyclic esters and carbonates.[14] While the pioneering study of Nederberg et al. discovered TBD's capability to produce random P(TMC-co-VL) copolymers (TMC : VL = 50 : 50) by solvent-free one-pot synthesis,[28] the ROCOP course of these two monomers has not been explored. Therefore, in this work, the conversion rates of TMC and δ-VL and the dependence of copolymer microstructure on TBD monomer selectivity were evaluated. Furthermore, two series of random poly(ester-carbonates) with various comonomer ratios were successfully synthesized using TBD/BnOH and TBD/mPEO-OH catalytic systems. The influence of the various obtained copolymer microstructures on thermal and mechanical properties was analyzed along with discussion of copolymers' possible bioapplications.

Simultaneous copolymerization of TMC and δ-VL (50 : 50 monomer ratio)

The TBD/BnOH (2 : 1) initiated copolymerizations of TMC and δ-VL (50 : 50 in the feed, 300 equiv. to BnOH) were conducted in a dichloromethane solution at room temperature. Aliquots were periodically withdrawn from the reaction mixture to monitor the conversion of comonomers and their incorporation into copolymer chains by ^1H NMR spectroscopy and SEC chromatography.

The copolymerization was determined to consist of two steps. In the first step, two types of polymerization centers were present: one that promoted the homoaddition of TMC and one without the preference. Upon complete TMC monomer conversion the reaction proceeded into the second step, in

which the propagation reaction of δ-VL competed with the transesterification reactions, producing random copolymers. Multiple results supported this assumption (Scheme 1).

It is clearly seen in Scheme 1a that TMC polymerized faster than δ-VL, reaching 59% conversion after 2 min and >99% conversion within 13 min. The conversion of δ-VL reached 22% after 2 min and 85% upon termination (60 min). The SEC traces for almost all products were bimodal without low-molar mass peaks, suggesting that oligomeric cyclic products were not formed (Scheme 1d). It was assumed from the distribution curves' character that two types of polymerization centers were present in the system. The first type indicated by a lower-molecular peak preferentially promoted homoaddition of TMC molecules producing almost monomodal homopolymer chains with narrow distribution. The second type promoted addition of both monomers and creation of copolymer chains, as evidenced by a higher-molecular broad SEC peak. Upon complete conversion of the TMC monomer, the propagation reaction of δ-VL competed with the transesterification reactions of the copolymer chains, mainly intra- and interchain transfer reactions, likely leading to principally random copolymer microstructure. Transesterification reactions are not uncommon for TBD-catalyzed systems.[26,32,36] A similar phenomenon was observed in the work of Yan *et al.*, where transesterification reactions led to the transformation of block copolycarbonates into random copolymers.[37]

To verify this copolymerization mechanism the diads content and average TMC and VL sequence lengths were calculated (Scheme 1b and c). The percentage of TMC-VL and VL-TMC heterodiads remained approximately constant with increasing monomer conversion, eliminating the possibility of two separate homopolymers being present in the system. The content of TMC–TMC homodiads and the average TMC sequence length decreased with simultaneous increase in number of TMC α-end units as the monomer conversion increased. Along with the approximately constant heterodiad content, the results further supported the assumption, that the presence of intra- and interchain reactions leads to "randomization" of the copolymer backbone.

It is worth mentioning that apparent M_n of resulting copolymer corresponded well with the theoretical one calculated from the comonomer feed (37 : 31 kg mol^{-1}) and the product possessed monomodal distribution with $Đ = 1.58$ after 60 min of polymerization (Scheme 1d).

Synthesis and microstructure of copolymers with various TMC : VL ratios

Encouraged by the successful preparation of random P(TMC-*co*-VL) copolymer after 60 min one pot synthesis, two series of random copolymers with varying molar ratios of TMC and VL were synthesized using BnOH and mPEO-OH as an initiator and macroinitiator, respectively. The overall results are summarized in Table 1 (for NMR spectra refer to Fig. S1–S3†). The molar ratios of TMC and VL units incorporated into the chains of resulting poly(ester-carbonates) were in good agreement with the initial feed ratios for both series. The copolymers had M_n in the range of 12–42 kg mol^{-1} and $Đ$ of 1.17–1.88. The random copolymerizations were moderately controlled due to transesterifications occurring at high δ-VL conversions. Copolymers produced on mPEO-OH macroinitiator possessed slightly narrower distributions than the BnOH-initiated ones. This can be ascribed to higher flexibility of the PEO-OH chain ends
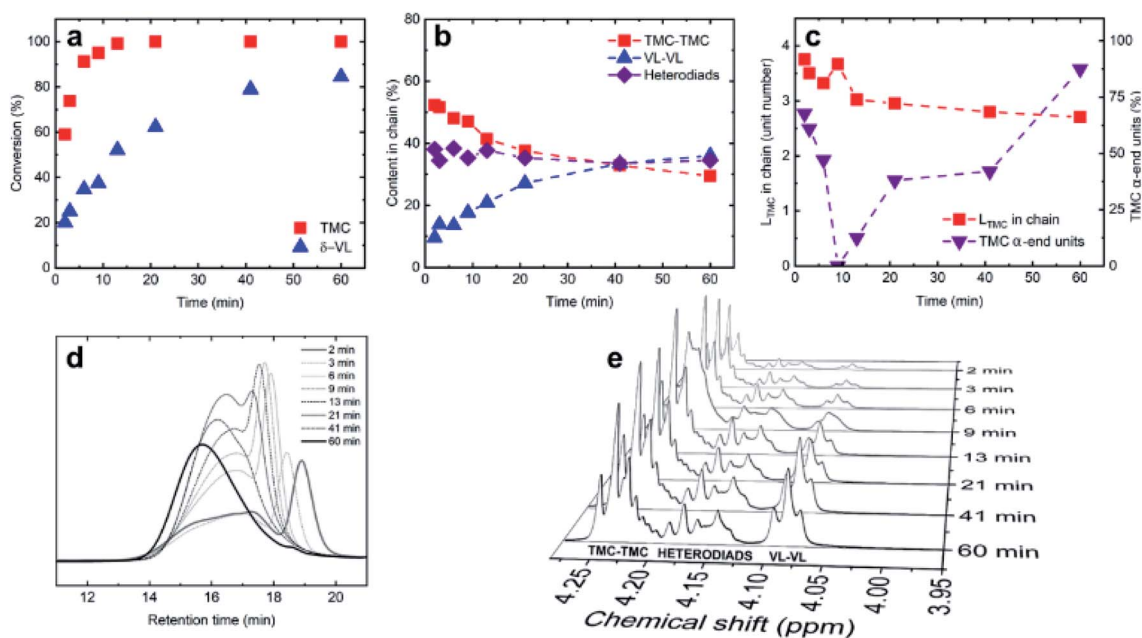
Scheme 1 Copolymerization of TMC and δ-VL initiated by TBD/BnOH (50 : 50 monomer feed ratio, DCM, 60 min, 25 °C); (a) conversion progress with time; (b) the evolution of homo- and heterodiad content in polymer chains with time; (c) the evolution of TMC segment length compared to TMC unit chain end groups; (d) SEC chromatograms of copolymers with time, (e) ^{1}H NMR spectra: the change in homo- and heterodiad peak intensity with time.

Table 1 Ring-opening copolymerizations of TMC initiated by BnOH/mPEO-OH and TBD[a]

Sample no.	TMC : VL[b] (mol%)	TMC : VL[c] (mol%)	TMC : VL L_A[d]	Conversion TMC : VL (%)	M_n^{theor} (kg mol^{-1})	$M_n(NMR)$[e] (kg mol^{-1})	$M_n(SEC)$[f] (kg mol^{-1})	Đ[f]
Random copolymers								
PVL	0 : 100	0 : 100	0 : 250	>99	34.4	25.0	25.1	1.17
C1	20 : 80	21 : 79	1.5 : 6.4	>99 : 98	54.1	n.d.	41.6	1.64
C2	50 : 50	47 : 52	2.5 : 3.0	>99 : 99	17.8	n.d.	21.1	1.64
C3	80 : 20	73 : 27	3.9 : 1.8	>99 : >99	30.0	n.d.	24.0	1.88
PTMC	100 : 0	100 : 0	376 : 0	>99	30.7	n.d.	38.4	1.58
PEO-*b*-random copolymers								
PEO-*b*-PVL	0100	0 : 100	0 : 323	99	32.5	37.0	21.7	1.46
PC1	20 : 80	21 : 79	1.6 : 6.9	>99 : 97	29.1	29.2	34.7	1.41
PC2	25 : 75	29 : 71	1.9 : 5.2	>99 : 99	23.7	24.1	27.4	1.60
PC3	50 : 50	46 : 54	2.7 : 3.5	>99 : 97	28.0	33.6	32.6	1.53
PC4	75 : 25	65 : 35	3.1 : 1.8	>99 : 99	32.1	15.6	32.6	1.56
PC5	80 : 20	76 : 24	4.9 : 1.7	>99 : 98	28.4	30.1	27.3	1.51
PEO-*b*-PTMC	100 : 0	100 : 0	397 : 0	>99	30.0	40.5	12.1	1.81

[a] Conditions: DCM solution (2.5 M), 2 : 1 TBD : BnOH/mPEO-OH, room temperature, 60 min. [b] mol% of TMC and VL in the feed. [c] mol% of TMC and VL in copolymer chains determined by ^{1}H NMR spectroscopy (CDCl$_3$). [d] Determined by ^{1}H NMR spectroscopy (CDCl$_3$). For the PEO-*b*-P(TMC-*co*-VL) copolymers, the number was determined for the P(TMC-*co*-VL) block. [e] Number-average molar mass calculated from data obtained by ^{1}H NMR spectroscopy (CDCl$_3$). [f] Apparent number-average molar mass and dispersity Đ determined by SEC analysis with RI detector, based on polystyrene standards.

compared to BnOH resulting in shorter contact time between the initiator and TBD. Similar phenomenon was reported by Guillerm *et al.*[38] for TBD-catalyzed copolymerizations of ε-caprolactone and L-/D,L-lactide utilizing 1-pyrenemethanol and mPEO-OH as an initiator and macroinitiator, respectively.

The data obtained by ATR FTIR spectroscopy further supported the assumption that the copolymerization procedure produced solely copolymers, not a mixture of homopolymers (Table S1 and Fig. S4†). Since Nederberg *et al.*[28] suggested that the blend of PVL and PTMC are immiscible, the FTIR spectrum of a homopolymers' blend would exhibit bands of both PVL and PTMC without significant broadening or shift in wavenumbers due to the absence of interactions, mainly hydrogen-bonding, as reported in the literature.[39–42] However, for our samples, this was not the case. All copolymers had a single >C=O stretching band located at wavenumbers between 1742 cm^{-1} (PTMC homopolymer) and 1730 cm^{-1} (PVL homopolymer) indicating the presence of both TMC and VL monomeric units in the chains. Similar behavior was observed for the bands corresponding to the O–C–C asymmetric stretching of both the

Table 2 Thermal properties of copolymers

Sample no.	TMC : VL L_A[a]	T_g[b] (°C)	T_m[c] (°C)	ΔH_m[c] (J g^{-1})	T'_m[d] (°C)	$\Delta H'_m$[c] (J g^{-1})	X_{cVL}[e] (%)	X_{cPTMC}[e] (%)	X_{cPEO}[e] (%)
Random copolymers									
PVL	**0 : 250**	−54	64	35	—	—	46	—	
C1	1.5 : 6.4	−46	53	47	47/51	36	20	—	
C2	2.5 : 3.0	−43	37	15	34	3	1	—	
C3	3.9 : 1.8	−30	—	—	—	—	—	—	
PTMC	**372 : 0**	−21	44	39	—	—	—	n.d.[f]	
PEO-*b*-random copolymers									
PEO-*b*-PVL	0 : 369	—	39/60	80	34/58	1/55	38[g]	—	1[g]
PC1	1.6 : 6.5	−47	55	57	50	52	17[g]	—	1[g]
PC2	1.8 : 4.8	−53	34/48/55	60	39/51	51	n.d.	n.d.	n.d.
PC3	2.6 : 3.5	−47	50	31	35/49	1/2	n.d.	n.d.	n.d.
PC4	3.1 : 1.8	−42	57	41	49/55	37	—	—	6
PC5	4.7 : 1.7	−36	54	23	52	—	—	—	—
PEO-*b*-PTMC	397 : 0	−35	28/36/50	13	41	15	n.d.	n.d.[f]	n.d.

[a] Determined by ^{1}H NMR spectroscopy (CDCl$_3$). [b] Glass transition temperature, T_g was determined according to the 2nd heating run. [c] Melting temperature, T_m and heat of fusion ΔH_m were determined according to the 1st heating run. [d] Melting temperature, T'_m and heat of fusion $\Delta H'_m$ were determined according to 2nd heating run. [e] Determined from 2nd heating run. [f] Could not be determined due to lack of $\Delta H_{m_{TMC100\%}}$ in the literature. [g] Determined from crystallization heat of fusion ΔH_c.

carbonate and ester units (Fig. S4a and b†). The spectra of block copolymers exhibited a similar trend with the additional presence of the PEO ether linkage asymmetric C–O–C stretch around 1113 cm^{-1} (Fig. S4c and d†).

The complex characterization of the copolymers' supramolecular structure using DSC, WAXD and FT-IR showed the ability of the catalytic system to produce tailored copolymers with varying supramolecular structures by simply modifying the comonomer ratio in the feed (Table 2 and Fig. 1).

All copolymers showed only one glass transition temperature (T_g) in their DSC thermograms obtained in the first and second heating. The T_g values were in-between those of PVL (−54 °C) (Fig. S6†) and PTMC (−21 °C) homopolymers. The presence of a single T_g was in compliance with the proposed copolymerization mechanism, since PTMC and PVL homopolymers were shown to be immiscible in a blend displaying two respective T_g values in the DSC thermogram.[28]

The crystallization capability of the copolymers depended greatly on the comonomer ratio and this crystallization behavior was validated by all performed analyses (Fig. 1). TMC chain sequences, while capable of arrangement into an ordered structure by secondary crystallization,[43] did not apparently achieve sufficient sequence length (maximum average sequence was determined as $L_A = 3.9$) and did not have suitable conditions to undergo the secondary crystallization process. Also considering the fact that the respective homopolymers were reported to be immiscible[28] and thus are expected to crystallize in separated domains, the crystalline phase content seemed to depend solely on VL unit content in the chain.

Based on DSC, copolymers C1 and C2 containing 80 mol% and 50 mol% of VL respectively, were both semi-crystalline and exhibited melting endotherms (Table 2 and Fig. 1C) at 53 and 36 °C, respectively, while C3 was shown to be completely amorphous. The crystalline phase content in the copolymers decreased significantly from 20 to 1% with the increase of TMC mol% from 20 (C1) to 50% (C2).

In accordance with DSC, the WAXD diffraction patterns of the C1 and C2 copolymers contained diffraction maxima at 21.6° and 24.2° (2θ) (Fig. 1A). The maxima were assigned to the crystalline VL segments while TMC segments were considered as amorphous, since no maxima characteristic for the PTMC homopolymer crystalline domains at 15.8° and 26.0° were observed. The C3 copolymer containing only 20% of VL units was shown to be completely amorphous with its diffractogram containing only a prominent amorphous halo.

The spectra obtained by ATR FTIR spectroscopy also followed the trend. The presence of VL crystalline phase showed to be evidenced by the appearance of two bands around 953 and 915 cm^{-1} (Fig. 1B). The appearance was determined as a result of C–O–C bonds bending into the all-trans chain conformation upon crystallization and the subsequent resonance of the bond vibrations in the ordered structure, according to a similar phenomenon reported for semi-crystalline poly(ε-caprolactone) (PCL).[44,45] The peaks were clearly present in the PVL homopolymer and C1 copolymer spectra. For the C2 copolymer with much lower crystalline phase content, the intensity of the bond vibration resonance was presumably too weak to exhibit in the spectrum. To our knowledge, the assignment to the two peaks to the VL crystalline phase content has not been reported before.

The added PEO block was capable of crystallization in all block copolymers (PC1–PC5, Table 2 and Fig. S5†). However, while its addition did not seem to significantly influence the P(TMC-co-VL) blocks' supramolecular structure, the precise determination of the crystalline phase content by DSC was obstructed by the similar melting temperatures of PVL and PEO crystalline phases (around 60 and 61 °C, respectively)[46,47] and will be evaluated in our further work.

Structure mechanical properties relationship

To evaluate the influence of varying microstructure on mechanical properties, the copolymers were solvent-cast into films. The film preparation was successful for samples C1, PC1
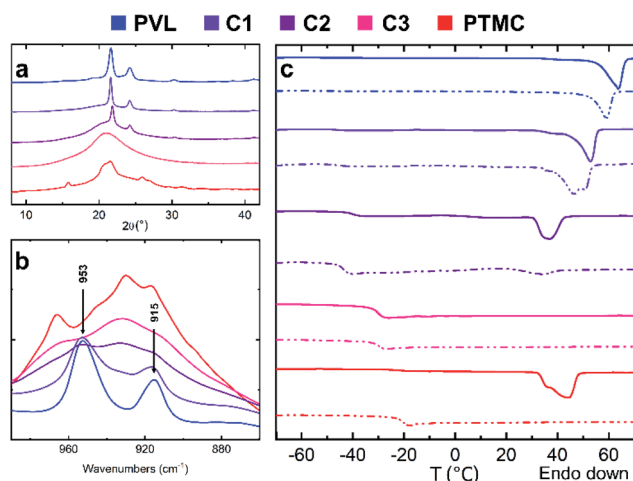

Fig. 1 Supramolecular structure characterization of synthesized P(TMC-co-VL) random copolymers; (a) WAXD patterns; (b) ATR-IR spectra, CH$_2$ rocking, C–C, O–C stretching region 990 to 860 cm^{-1}; (c) DSC thermograms, solid line = 1st heating, dash line = 2nd heating.
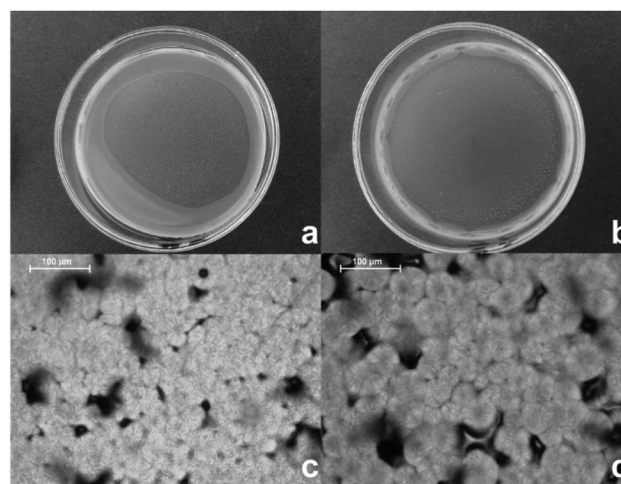

Fig. 2 Spherulite formation in copolymer samples; copolymer films of (a) C1 copolymer, (b) PC1 copolymer, polarized optical micrographs of (c) C1 copolymer, (d) PC1 copolymer.

and PC3, for which the crystallinity degree significantly influenced the resulting morphology. Films prepared from semicrystalline copolymers C1 and PC1 were opaque with a clear presence of small spherulites, while that obtained from the *de facto* amorphous PC3 copolymer remained purely opaque. The images of C1/PC1 films are presented in Fig. 2. Both films consisted of spherulite clusters with similar morphology and a discontinuous amorphous phase. Smaller sized C1 spherulites can be explained by the increased nucleation rate for the C1 sample opposed to PC1 due to its higher molar mass in accordance with published study on crystallizations of PCL with varying molar masses.[48]

The failure to obtain a cohesive film from the remaining copolymers was due to their waxy character, resulting from higher TMC unit content. For sample C2 with identical TMC : VL ratio as sample PC3, the film-forming capability was hindered by lower molar mass and higher degree of randomness.[48]

Films were cut into testing specimens and subjected to uniaxial stress–strain measurements, to evaluate their tensile properties, either directly or after 48 h incubation with SBF at 37 °C as a model biological fluid to analyze the influence of aqueous buffers. Dynamic mechanical properties of untreated samples were evaluated by dynamic mechanical analysis. The results were compared to properties of PVL homopolymer and PEO-*b*-PVL copolymer tested at the same conditions.

The obtained stress–strain curves of untreated samples clearly indicated that the TMC : VL chain ratio had a considerable impact on tensile properties (Scheme 2). The difference between mechanical behavior of homopolymers, PVL and PTMC is substantial. PVL is a semi-crystalline thermoplastic

similar to PCL,[49,50] while PTMC is an elastomer, tough and highly flexible at molar masses over 100 kg mol^{-1}.[51] Based on the results, copolymers containing 20% of TMC units (C1, PC1) displayed the properties of both homopolymers. While their tensile strength (TS) and Young's modulus (E) were reduced opposed to PVL, their elongation at break (ε_b) increased dramatically. Specifically, for sample C1, TS and E were reduced by 7 and 181 MPa, respectively, while its ε_b increased from 26 to 590% by 2200%. The behavior was attributed to the C1 microstructure, which was shown to consist mainly of an amorphous phase with small, separated domains of crystalline VL segments. These crystalline segments can act as a physical crosslinker and absorb deformation energy, resulting in a tougher material,[52] while the amorphous phase provides flexibility.

The stress–strain curve character further supported the suggestion that crystalline VL segments act as physical crosslinkers. The curves exhibited linear response to strain at low elongations with smooth transitions from the elastic to the plastic flow region. This behavior is characteristic for loosely crosslinked rubbers.[53] Furthermore, the results obtained for the PC3 sample with 50% TMC units were in compliance with the suggestion. Missing a significant crystalline phase to act as a crosslinker, its mechanical properties were considerably poorer, even though the PC1 and PC3 copolymers had comparable molar masses. The low flexibility of the PC3 copolymer despite its high TMC content was explained by the lower molar mass of the TMC segments, since in order to obtain a highly flexible PTMC material, a higher molar mass needs to be achieved.[51]

Although the presence of the PEO block in the PC1 copolymer seemed to have a negligible impact on the copolymer tensile properties of untreated samples, its influence considerably increased for samples incubated with SBF (Scheme 2). The appearance of all samples containing the PEO block appeared as milky white opposed to original clear or opaque, and their tensile properties significantly deteriorated compared to untreated specimens. For copolymers PEO-*b*-PVL and PC3 it was impossible to obtain relevant data. These results could be explained by the increase in degradation rate and water sorption in SBF for copolymers containing the hydrophilic PEO block, leading to deterioration of their tensile properties, since the specimens' thickness was only 0.1 mm. Further analysis of the incubated specimens by ATR FTIR spectroscopy has shown a decrease in intensity of the PEO asymmetric C–O–C stretching band around 1113 cm^{-1} (Fig. S7†), hinting at the possibility of the PEO blocks' dissolution in SBF resulting from the copolymer ester bond cleavage. The behavior of the samples was not entirely surprising, since PEO was reported to increase water sorption and degradation rate in aqueous buffers for PEO-*b*-PCL copolymers,[54–56] and recently reported to increase degradation rates in PEO/PCL blends exposed to SBF.[57] However, further thorough degradation analyses need to be performed to confirm these suggestions.

On the other hand, the appearance of more hydrophobic C1 copolymer samples resembled the untreated ones. Its tensile properties also remained similar with TS, E and ε_b being
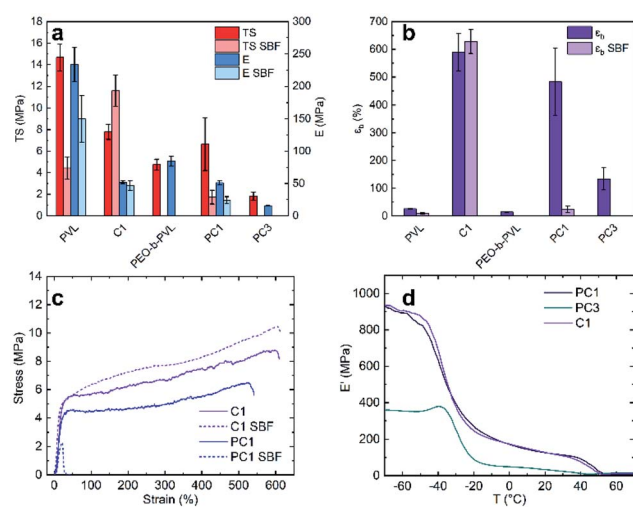
Scheme 2 Tensile and dynamic mechanical properties of representative PVL, PEO-*b*-PVL, P(TMC-*co*-VL) and PEO-*b*-P(TMC-*co*-VL); (a) tensile strength and Young's modulus before and after incubation with SBF; missing data indicate the specimens could not be evaluated, (b) elongation at break before and after incubation with SBF; missing data indicate the specimens could not be evaluated, (c) representative stress–strain curves of synthesized copolymers before and after incubation with SBF, (d) the dependency of copolymer storage modulus E' on temperature.

12 MPa, 47 MPa and 628%, respectively. The results weren't unexpected, since the degradation of hydrophobic poly(ester-carbonates) is slower and in order to observe a significant deterioration of mechanical properties a long-term analysis needs to be conducted.[58,59]

Temperature-dependence of storage moduli E' analyzed by DMA for representative copolymers is plotted in Scheme 2. All samples exhibited a decline in E' upon glass transition followed by a rubbery plateau and a terminal flow region. The obtained data followed the data from tensile testing. The C1 and PC1 copolymers displayed similar dynamic behavior and their curves resembled those of loosely cross-linked rubbers and elastomers thanks to the presence of crystalline domains functioning as physical crosslinkers.[60,61] Compared to PC3 copolymer they exhibited higher value of E' and their terminal flow region shifted towards slightly higher temperatures. Comparable results were reported by Ryynänen et al. for multiblock poly(ε-caprolactone-co-D,L-lactide-b-ε-caprolactone) (P(CL/DLLA-b-CL)) copolymers[62] Similarly to the evaluation of tensile properties, based on the negligible difference of PC1 and PC3 copolymers' molar masses, the difference in dynamic mechanical behavior was directly linked to the influence of crystalline phase content arising from their copolymer microstructure.

Additionally, the influence of copolymer microstructure on T_g was clearly proved according to maxima of loss modulus E'' and damping ($\tan \delta$). The height of the $\tan \delta$ peak at T_g ($h(\tan \delta)$) is reported here as a measure of the magnitude of transition (Table 3 and Fig. S8†). All three samples exhibited a single T_g, characteristic for random copolymers, where the C1 and PC1 copolymers displayed almost identical values whereas the increased TMC : VL unit ratio of PC3 sample shifted its T_g towards higher temperatures.

When compared to values obtained by DSC the T_g values were higher. This discrepancy can be ascribed to the difference in operating principles of the analyses and their varying sensitivity to different degrees of chain mobility as it was reported in literature.[63–65]

In accordance with previous results, the presence of crystalline phase acting as a crosslinker influenced the height of $\tan \delta$ peaks corresponding to T_g, $h(\tan \delta)$, which has been reported to decrease with increasing crosslink density and E'.[60,61,66] The $h(\tan \delta)$ for C1 and PC1 peaks has decreased by more than 50% compared to the $h(\tan \delta)$ of amorphous sample PC3. While this trend is usually accompanied by the increase of T_g,[60] it was not observed for our copolymers, presumably because the copolymers differed in the TMC : VL unit ratio and thus their T_g were not comparable. Similar results were

obtained by Helminen et al., who studied dynamic behavior of crosslinked poly(ε-caprolactone/D,L-lactide) copolymers with different ε-caprolactone/D,L-lactide unit ratios and crosslink density.[61]

Overall, it was demonstrated that when utilizing TBD-based catalytic systems, it is possible to obtain P(TMC-co-VL) copolymers with dramatically different mechanical properties via one-pot procedure by simply adjusting the comonomer ratio in the reaction feed. Considering their biocompatibility[51,67,68] and biodegradability,[69–71] these materials could be highly suitable for soft tissue engineering, where the material's mechanical properties should match those of the tissue as much as possible,[72] or drug delivery. The C1 and PC1 copolymers exhibited properties comparable to previously reported biodegradable thermoplastic elastomers.[73,74] The C1 copolymer retained these properties after incubation with SBF. Its tensile strength (TS = 12 MPa) and Young's modulus (E = 47 MPa) were specifically comparable to human cartilage,[75] and thus could be potentially suitable for cartilage regeneration. Lower-molecular weight poly(ester-carbonates) with higher TMC content could be utilized as drug delivery systems.[76] Same application could be suitable for PEO block-containing copolymers, due to the known benefits of the PEO shell for evading the immune system.[77]

Conclusions

We have successfully prepared two series of P(TMC-co-VL) and PEO-b-P(TMC-co-VL) copolymers with versatile microstructure and properties by simply tailoring the ratio of TMC and δ-VL in the copolymerization feed. By first focusing our attention on the copolymerization mechanism and its influence over copolymer microstructure we were able to produce copolymers with up to 628% elongation at break that could be potentially suitable for a wide spectrum of biomedical applications. To our best knowledge, this is the first time attention was focused on the copolymerization mechanism of TMC and δ-VL using TBD as a catalyst. We believe that our findings could be useful for the design of advanced copolymers with specific requirements for in vivo degradation rate or mechanical properties. Furthermore, the simplicity and effectiveness of the TBD-catalyzed one-pot synthesis leads us to believe that this procedure could be advantageous for larger scale syntheses of application-tailored copolymers without the need for metal complexes. In our future work, we plan to fully explore the copolymers' potential in specific bioapplications with focus on obtaining high molar mass thermoplastic elastomers suitable for 3D scaffold printing and the utilization of the soft elastomers for targeted drug delivery systems with tailorable degradation speed.

Conflicts of interest

There are no conflicts to declare.

Acknowledgements

Table 3 Copolymer glass transitions obtained from DMA vs. DSC

Sample no.	T_g (E'') (°C)	T_g($\tan \delta$) (°C)	$h(\tan \delta)$	T_g(DSC) (°C)
C1	−36	−31	0.17	−46
PC1	−36	−30	0.19	−47
PC3	−29	−23	0.41	−47

Notes and references

1 N. Iqbal, A. S. Khan, A. Asif, M. Yar, J. W. Haycock and I. U. Rehman, *Int. Mater. Rev.*, 2019, **64**, 91–126.

2 R. P. Brannigan and A. P. Dove, *Biomater. Sci.*, 2017, **5**, 9–21.

3 C. Liu, Z. Xia and J. T. Czernuszka, *Chem. Eng. Res. Des.*, 2007, **85**, 1051–1064.

4 F. Zhang and M. W. King, *Adv. Healthcare Mater.*, 2020, **9**, 1901358.

5 J.-Z. Wang, M.-L. You, Z.-Q. Ding and W.-B. Ye, *Mater. Sci. Eng. C*, 2019, **97**, 1021–1035.

6 A. P. Pêgo, A. A. Poot, D. W. Grijpma and J. Feijen, *J. Biomater. Sci. Polym. Ed.*, 2001, **12**, 35–53.

7 A. P. Pêgo, A. A. Poot, D. W. Grijpma and J. Feijen, *Macromol. Biosci.*, 2002, **2**, 411–419.

8 C. L. A. M. Vleggeert-Lankamp, J. Wolfs, A. P. Pêgo, R. v. d. Berg, H. Feirabend and E. Lakke, 2008, **109**, 294.

9 L. R. Pires, V. Guarino, M. J. Oliveira, C. C. Ribeiro, M. A. Barbosa, L. Ambrosio and A. P. Pego, *J. Tissue Eng. Regener. Med.*, 2016, **10**, E154–E166.

10 A. Güney, J. Malda, W. J. Dhert and D. W. Grijpma, *Int. J. Artif. Organs*, 2017, **40**, 176–184.

11 D. N. Rocha, P. Brites, C. Fonseca and A. P. Pêgo, *PLoS One*, 2014, **9**, e88593.

12 M. C. Tanzi, P. Verderio, M. G. Lampugnani, M. Resnati, E. Dejana and E. Sturani, *J. Mater. Sci. Mater. Med.*, 1994, **5**, 393–396.

13 A. Stjerndahl, A. Finne-Wistrand, A. C. Albertsson, C. M. Bäckesjö and U. Lindgren, *J. Biomed. Mater. Res., Part A*, 2008, **87**, 1086–1091.

14 Q. L. Song, S. Y. Hu, J. P. Zhao and G. Z. Zhang, *Chin. J. Polym. Sci.*, 2017, **35**, 581–601.

15 S. Naumann, P. B. V. Scholten, J. A. Wilson and A. P. Dove, *J. Am. Chem. Soc.*, 2015, **137**, 14439–14445.

16 X. Wang, J. Liu, S. Xu, J. Xu, X. Pan, J. Liu, S. Cui, Z. Li and K. Guo, *Polym. Chem.*, 2016, **7**, 6297–6308.

17 K. Zhang, Q. Fu, J. Yoo, X. Chen, P. Chandra, X. Mo, L. Song, A. Atala and W. Zhao, *Acta Biomater.*, 2017, **50**, 154–164.

18 A. P. Dove, *ACS Macro Lett.*, 2012, **1**, 1409–1412.

19 S. Paul, Y. Zhu, C. Romain, R. Brooks, P. K. Saini and C. K. Williams, *Chem. Commun.*, 2015, **51**, 6459–6479.

20 S. Hu, J. Zhao, G. Zhang and H. Schlaad, *Prog. Polym. Sci.*, 2017, **74**, 34–77.

21 J. Zhao, D. Pahovnik, Y. Gnanou and N. Hadjichristidis, *Macromolecules*, 2014, **47**, 3814–3822.

22 P. Olsén, K. Odelius, H. Keul and A.-C. Albertsson, *Macromolecules*, 2015, **48**, 1703–1710.

23 J. Simon, J. V. Olsson, H. Kim, I. F. Tenney and R. M. Waymouth, *Macromolecules*, 2012, **45**, 9275–9281.

24 K. Makiguchi, Y. Ogasawara, S. Kikuchi, T. Satoh and T. Kakuchi, *Macromolecules*, 2013, **46**, 1772–1782.

25 A. Couffin, D. Delcroix, B. Martín-Vaca, D. Bourissou and C. Navarro, *Macromolecules*, 2013, **46**, 4354–4360.

26 M. Fèvre, J. Vignolle, Y. Gnanou and D. Taton, in *Polymer Science: A Comprehensive Reference*, ed. K. Matyjaszewski

and M. Möller, Elsevier, Amsterdam, 2012, pp. 67–115, DOI: 10.1016/B978-0-444-53349-4.00119-9.

27 S. Naumann, in *Organic Catalysis for Polymerisation*, The Royal Society of Chemistry, 2019, pp. 121–197, DOI: 10.1039/9781788015738-00121.

28 F. Nederberg, B. G. G. Lohmeijer, F. Leibfarth, R. C. Pratt, J. Choi, A. P. Dove, R. M. Waymouth and J. L. Hedrick, *Biomacromolecules*, 2007, **8**, 153–160.

29 I. Nifant'ev, A. Shlyakhtin, V. Bagrov, B. Lozhkin, G. Zakirova, P. Ivchenko and O. Legon'kova, *React. Kinet. Mech. Catal.*, 2016, **117**, 447–476.

30 G. W. Fahnhorst and T. R. Hoye, *ACS Macro Lett.*, 2018, **7**, 143–147.

31 M. Xiong, D. K. Schneiderman, F. S. Bates, M. A. Hillmyer and K. Zhang, *Proc. Natl. Acad. Sci. U. S. A.*, 2014, **111**, 8357–8362.

32 R. C. Pratt, B. G. G. Lohmeijer, D. A. Long, R. M. Waymouth and J. L. Hedrick, *J. Am. Chem. Soc.*, 2006, **128**, 4556–4557.

33 J. Ling, W. Zhu and Z. Shen, *Macromolecules*, 2004, **37**, 758–763.

34 A. P. Pêgo, Z. Zhong, P. J. Dijkstra, D. W. Grijpma and J. Feijen, *Macromol. Chem. Phys.*, 2003, **204**, 747–754.

35 T. Kokubo and H. Takadama, *Biomaterials*, 2006, **27**, 2907–2915.

36 B. G. G. Lohmeijer, R. C. Pratt, F. Leibfarth, J. W. Logan, D. A. Long, A. P. Dove, F. Nederberg, J. Choi, C. Wade, R. M. Waymouth and J. L. Hedrick, *Macromolecules*, 2006, **39**, 8574–8583.

37 B. Yan, J. Hou, C. Wei, Y. Xiao, M. Lang and F. Huang, *Polym. Chem.*, 2020, **11**, 2166–2172.

38 B. Guillerm, V. Lemaur, B. Ernould, J. Cornil, R. Lazzaroni, J.-F. Gohy, P. Dubois and O. Coulembier, *RSC Adv.*, 2014, **4**, 10028–10038.

39 Y. Xu, C. Wang, N. M. Stark, Z. Cai and F. Chu, *Carbohydr. Polym.*, 2012, **88**, 422–427.

40 C. Vogel, E. Wessel and H. W. Siesler, *Biomacromolecules*, 2008, **9**, 523–527.

41 T. A. Vida, A. C. Motta, A. R. Santos Jr., G. B. C. Cardoso, C. C. d. Brito and C. A. d. C. Zavaglia, *Mater. Res.*, 2017, **20**, 910–916.

42 D. I. Bower, *An Introduction to Polymer Physics*, Cambridge University Press, Cambridge, 2002.

43 L. Reinišová, F. Novotný, M. Pumera, K. Kološtová and S. Hermanová, *Macromol. Res.*, 2018, **26**, 1026–1034.

44 K. Phillipson, J. N. Hay and M. J. Jenkins, *Thermochim. Acta*, 2014, **595**, 74–82.

45 V. N. Nikitin and B. Z. Volchek, *Russ. Chem. Rev.*, 1968, **37**, 225–242.

46 Y. Furuhashi, P. Sikorski, E. Atkins, T. Iwata and Y. Doi, *J. Polym. Sci., Part B: Polym. Phys.*, 2001, **39**, 2622–2634.

47 W. Wang, X. Yang, Y. Fang, J. Ding and J. Yan, *Appl. Energy*, 2009, **86**, 1479–1483.

48 H.-L. Chen, L.-J. Li, W.-C. Ou-Yang, J. C. Hwang and W.-Y. Wong, *Macromolecules*, 1997, **30**, 1718–1722.

49 F. Le Devedec, H. Boucher, D. Dubins and C. Allen, *Mol. Pharm.*, 2018, **15**, 1565–1577.

50 K. Ragaert, I. De Baere, L. Cardon and J. Degrieck, 2014.

51 A. P. Pêgo, D. W. Grijpma and J. Feijen, *Polymer*, 2003, **44**, 6495–6504.

52 S. Liow, V. Lipik, L. Widjaja, S. Venkatraman and M. Abadie, *Express Polym. Lett.*, 2011, **5**, 897–910.

53 G. R. Hamed and N. Rattanasom, *Rubber Chem. Technol.*, 2002, **75**, 323–332.

54 W. Shen-Guo and Q. Bo, *Polym. Adv. Technol.*, 1993, **4**, 363–366.

55 J.-Z. Bei, J.-M. Li, Z.-F. Wang, J.-C. Le and S.-G. Wang, *Polym. Adv. Technol.*, 1997, **8**, 693–696.

56 S. Li, H. Garreau, M. Vert, T. Petrova, N. Manolova and I. Rashkov, *J. Appl. Polym. Sci.*, 1998, **68**, 989–998.

57 A. I. Visan, G. Popescu-Pelin, O. Gherasim, A. Mihailescu, M. Socol, I. Zgura, M. Chiritoiu, L. Elena Sima, F. Antohe, L. Ivan, D. M. Vranceanu, C. M. Cotruţ, R. Cristescu and G. Socol, *Polymers*, 2020, **12**, 717.

58 L. Yang, J. Li, S. Meng, Y. Jin, J. Zhang, M. Li, J. Guo and Z. Gu, *Polymer*, 2014, **55**, 5111–5124.

59 A. P. Pêgo, A. A. Poot, D. W. Grijpma and J. Feijen, *J. Controlled Release*, 2003, **87**, 69–79.

60 J. Diez, R. Bellas, J. López, G. Santoro, C. Marco and G. Ellis, *J. Polym. Res.*, 2009, **17**, 99.

61 A. O. Helminen, H. Korhonen and J. V. Seppälä, *Macromol. Chem. Phys.*, 2002, **203**, 2630–2639.

62 T. Ryynanen, A. Nykanen and J. V. Seppala, *Express Polym. Lett.*, 2008, **2**, 184–193.

63 L. Wang, Z. Zhang, H. Chen, S. Zhang and C. Xiong, *J. Polym. Res.*, 2009, **17**, 77.

64 F. Rezgui, M. Swistek, J. M. Hiver, C. G'Sell and T. Sadoun, *Polymer*, 2005, **46**, 7370–7385.

65 M. T. Kalichevsky, E. M. Jaroszkiewicz, S. Ablett, J. M. V. Blanshard and P. J. Lillford, *Carbohydr. Polym.*, 1992, **18**, 77–88.

66 N. Warasitthinon and C. G. Robertson, *Rubber Chem. Technol.*, 2018, **91**, 577–594.

67 C. Ulker, Z. Gok and Y. Guvenilir, *J. Renewable Mater.*, 2019, **7**, 335–343.

68 J. Liu, C. Zhang, Z. Li, L. Zhang, J. Xu, H. Wang, S. Xu, T. Guo, K. Yang and K. Guo, *Eur. Polym. J.*, 2019, **113**, 197–207.

69 L. Reinišová, L. Artigues, P. Lovecká, Z. Sofer and S. Hermanová, *presented in part at the Czech-Slovak Conference POLYMERS 2018 Třešť*, 2018.

70 K. Fukushima, *Biomater. Sci.*, 2016, **4**, 9–24.

71 A. Nakayama, N. Kawasaki, Y. Maeda, I. Arvanitoyannis, S. Aiba and N. Yamamoto, *J. Appl. Polym. Sci.*, 1997, **66**, 741–748.

72 C. F. Guimarães, L. Gasperini, A. P. Marques and R. L. Reis, *Nat. Rev. Mater.*, 2020, **5**, 351–370.

73 Y. Huang, R. Chang, L. Han, G. Shan, Y. Bao and P. Pan, *ACS Sustainable Chem. Eng.*, 2016, **4**, 121–128.

74 Z. Jing, X. Shi and G. Zhang, *Polym. Int.*, 2017, **66**, 1487–1497.

75 *Tissue Eng., Part B*, 2011, **17**, 213–227.

76 Y. Yeo, *Nanoparticulate drug delivery systems: strategies, technologies, and applications*, John Wiley & Sons, 2013.

77 M. L. Adams, A. Lavasanifar and G. S. Kwon, *J. Pharm. Sci.*, 2003, **92**, 1343–1355.